

日本原子力研究開発機構機関リポジトリ
Japan Atomic Energy Agency Institutional Repository

Title	Intermetallic charge transfer in FeTiO ₃ probed by resonant inelastic soft x-ray scattering
Author(s)	Akane Agui, Takayuki Uozumi, Masaichiro Mizumaki, Tanel Käämbre
Citation	Physical Review B, 79(9), 092402 (2009)
Text Version	Publisher
URL	http://jolissrch-inter.tokai-sc.jaea.go.jp/search/servlet/search?5018830
DOI	http://dx.doi.org/10.1103/PhysRevB.79.092402
Right	©2009 The American Physical Society

Intermetallic charge transfer in FeTiO₃ probed by resonant inelastic soft x-ray scattering

Akane Agui*

Synchrotron Radiation Research Center, Japan Atomic Energy Agency, SPring-8, 1-1-1 Kouto, Sayo-cho, Sayo-gun, Hyogo 679-5148, Japan

Takayuki Uozumi

Osaka Prefecture University, 1-1 Gakuen-cho, Sakai-shi, Osaka 599-8531, Japan

Masaichiro Mizumaki

Japan Synchrotron Radiation Research Institute, SPring-8, 1-1-1 Kouto, Sayo-cho, Sayo-gun, Hyogo 679-5198, Japan

Tanel Käämbre

Institute of Physics, Tartu University, Riia 142 EE-51014 Tartu, Estonia

(Received 3 June 2008; revised manuscript received 13 February 2009; published 11 March 2009)

Resonant inelastic soft x-ray inelastic-scattering (RIXS) spectra of single-crystal iron ilmenite FeTiO₃ were measured at the Ti 2*p* resonance, and additional peaks at -2.5 and -4.5 eV in energy loss were observed. In order to investigate the origin of these peaks, we performed a double-cluster model calculation based on full-multiplet calculation in which, in addition to the interaction with the O 2*p* ligands of the Ti ion, which is already included in the more conventional single-cluster model, the charge-transfer contribution to Ti 3*d* from Fe 3*d* is taken into account. The calculation shows that the peaks may be attributed to the Fe 3*d* → Ti 3*d* intermetallic charge-transfer scheme that previously had not been accounted for in RIXS.

DOI: [10.1103/PhysRevB.79.092402](https://doi.org/10.1103/PhysRevB.79.092402)

PACS number(s): 75.50.Lk, 78.20.Bh, 78.70.En

Ilmenite FeTiO₃ is a typical parent material for a spin frustration system.¹ In FeTiO₃, Fe is divalent (Fe²⁺, *d*⁶) and Ti is tetravalent (Ti⁴⁺, *d*⁰). Fe and Ti ions occupy the basal cation planes alternatively. The local symmetry around the transition-metal ions, both Fe and Ti, has *D*_{3*d*} symmetry. In this study, we primarily investigate the characteristics of energy-loss peaks that we experimentally observed at -2.5 and -4.5 eV in the Ti 2*p* resonant inelastic soft x-ray inelastic scattering (RIXS) of FeTiO₃. The interpretation of the data is given using model calculations, which indicate that direct intermetallic charge transfer is present and has similar rates to the more widely accepted cation-anion charge transfer.

The total electronic density spectrum of the occupied states is typically studied using photoelectron spectroscopy, which yields information of the chemical state and the band structure. However, x-ray emission spectroscopy (XES) has several advantages for studying the bulk properties of a material since the XES offers element and orbital specific occupied valence-band information from a probe depth in the 100 nm range. If resonant excitation is applied, the coherence of the excitation and the decay transitions makes proper the description as a second-order optical process, i.e., the RIXS. The resonant XES, or RIXS, goes one step further; for example, the dipole selection rules of such a second-order process allows one to investigate *d-d* excitations.

In an effort to acquire a detailed understanding and interpretation of the RIXS of transition metals (TMs) in TM compounds, particularly in oxides, theoretical studies have been strenuously progressed.² Considering the charge-transfer effects in the RIXS spectra, the single cluster (including the TM ion and its oxygen ligands) is usually seen as sufficient for an adequate description of the spectral features that arise in the TM RIXS. Both TiO₂ and FeTiO₃ are known as typical

*d*⁰ systems in which the tetravalent Ti ion is surrounded by neighboring oxygen ions in an octahedral configuration. In a straightforward picture, an interpretation of the Ti 2*p* RIXS must account for the sequence of $2p^63d^0 \rightarrow 2p^53d^1 \rightarrow 2p^63d^0$ states and the O 2*p*-Ti 3*d* charge transfer. A comparison of the experimental Ti 2*p* RIXS spectra of TiO₂ and FeTiO₃ draws attention to two minor peaks in the energy region between -2 and -5 eV below the elastic peak, which are present in the FeTiO₃ (Ref. 3) but not the TiO₂ (Ref. 4) spectra. However, the single-cluster calculation yields a theoretical spectrum that is void in this energy region even for FeTiO₃. Since the single-cluster model failed to reproduce the observed RIXS spectral structure, we have expanded the theoretical concept into a double-cluster (including, apart from the Ti with oxygen neighbors, an adjacent Fe ion with respective ligand oxygens) model calculation which, as seen below, gives a good account of the experimental results.

The RIXS and XAS measurements were carried out at the undulator beamline I511-3 at the MAX-II storage ring (MAX-lab National Laboratory, Lund University, Sweden). XAS at the Ti 2*p* edge was performed in the total electron yield mode and normalized to the photocurrent from a clean gold mesh. The RIXS spectra were recorded with a high-resolution grazing-incidence grating Rowland-mount spectrometer in which the energy resolution was set to be 0.4 eV.⁵ During the XAS and RIXS measurements, the energy resolution of the beamline monochromator was about 0.3 and 0.5 eV, respectively. The sample was a single crystal of FeTiO₃, which was grown by the floating-zone method¹ and cut such that the sample surface lies in the crystal *ab* plane; see inset of Fig. 1. The incident angle of the photon beam was about 20° to the sample surface and the polarization vector of the incident beam was 20° from the sample surface normal, i.e., along the crystal *c* axis. The spectrometer was oriented along

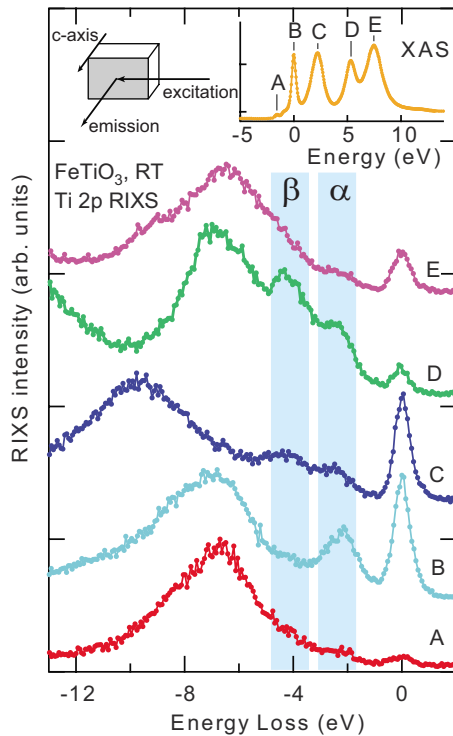


FIG. 1. (Color online) Experimental Ti $2p$ RIXS of single-crystalline FeTiO_3 , plotted on the energy-loss scale. The excitation photon energies A–E are indicated with bars above the XAS.

the polarization vector of the incident beam. Measurements were carried out at room temperature.

Figure 1 shows the measured Ti $2p$ RIXS of FeTiO_3 excited at various photon energies, which correspond to the absorption maxima (vertical bars labeled A–E of the XAS in the inset of Fig. 1). The RIXS spectra are plotted as a function of the energy loss, i.e., the incident energy position is set to be 0 eV of RIXS. The maximum peak intensity of each spectrum was set equal to 1. The spectral structure of XAS and the RIXS of the present study reproduces that found in the literature,³ and the fine peaks appear more clearly. The main XAS structure consists of four peaks, which arise from the spin-orbit splitting of the Ti $2p$ level and the crystal-field splitting of the Ti $3d$ level. Peaks B and D (C and E) were previously assigned, in the one-electron picture, to the e_g (t_{2g}) component of the crystal-field split $3d$ orbital.⁶ An additional peak appears at -4.5 eV (β) energy loss when the excitation energy is tuned at peak C. Earlier, Butorin *et al.*³ reported Ti $2p$ RIXS spectra of a natural mineral sample in which they found indications of a spectral feature at -2.5 eV energy loss, for which they proposed the d - d excitations (in the presence of Ti^{3+} arising from possible oxygen vacancies in the sample) as a plausible origin. In our present study, we used a single crystal of FeTiO_3 in order to be able to excite preferentially the electronic states along the crystal c axis and the sample was oriented accordingly. Consequently, the quality of the Ti $2p$ RIXS spectra was improved. The spectral feature at -2.5 eV energy loss (labeled α in Fig. 1) is readily distinguished, and an additional RIXS peak (labeled β) is observed at -4.5 eV energy loss. It has been reported that a small peak appears at about -2.5 eV energy loss in the

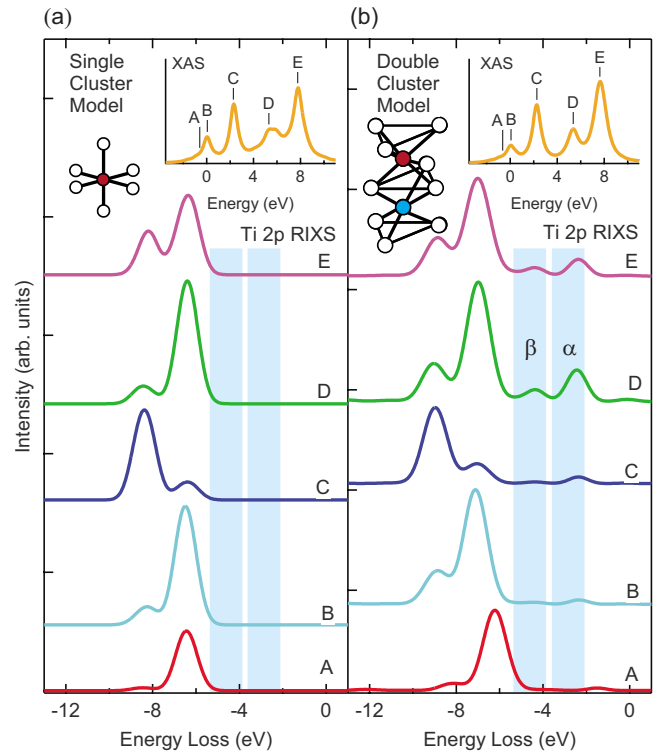


FIG. 2. (Color online) Calculated results of Ti $2p$ RIXS within (a) the single-cluster model and (b) the double-cluster model. The letters in the spectra correspond to the letters in Fig. 1. Spectra for model clusters TiO_6 and FeTiO_9 are shown in the inset: the open circles represent the oxygen ions and the solid circles represent the transition-metal ions.

Ti $2p$ RIXS of some titanium oxides, such as $\text{La}_x\text{Sr}_{1-x}\text{TiO}_3$ and nanoporous TiO_2 ,^{7–9} and that peak was attributed to a contribution from the Ti^{3+} ion. However, in the present case, the incident energy dependence of the peak is distinct, i.e., the present α and β peaks appear even when the excitation energies are low. Therefore, the origin of the α and β peaks of the Ti $2p$ RIXS of FeTiO_3 could not be attributed to the contribution of Ti^{3+} arising from stoichiometry. Their origin must be different.

In order to investigate the origin of the observed peaks at -2.5 and -4.5 eV of Ti $2p$ RIXS, we performed theoretical calculations based on two types of charge-transfer cluster models: the TiO_6 cluster and the FeTiO_9 cluster model, as shown in the inset of Figs. 2(a) and 2(b), respectively. The former type of cluster, TiO_6 , has conventionally been used in the analyses of soft x-ray spectra,² particularly for the Ti $2p$ RIXS analysis of TiO_2 .⁴ On the other hand, the latter type of cluster, FeTiO_9 , is introduced here to describe the structure in RIXS, which, as it will be shown, lies beyond the description of the classical TiO_6 cluster approach. As shown in the inset of Fig. 2(b), the Ti and Fe ions of the FeTiO_9 cluster share oxygen ions in a trigonal plane.

The model Hamiltonian for the TiO_6 cluster is taken to be a standard type in the conventional approach,⁴ and is given by

$$H = H_{\text{Ti}} + H_{\text{O}} + H_{\text{Ti-O}}, \quad (1)$$

where the terms describe the following interactions: H_{Ti} includes the Ti $3d$ level ϵ_d , crystal-field splitting $10Dq$ and the parameter $a [=Ed(a_{1g}) - Ed(e_g\pi)]$ for the $3d$ state, the $3d$ Coulomb repulsive energy U_{dd} , and the $2p$ core-hole potential U_{dc} , in addition to the full-multiplet interactions composed of the spin-orbit interaction for Ti $3d$ and $2p$ states and the multipole part of $3d$ - $3d$ and $3d$ - $2p$ Coulomb interaction. H_{O} describes the O $2p$ level ϵ_p , and $H_{\text{Ti-O}}$ describes the Ti $3d$ -O $2p$ hybridization, which is given in terms of transfer integrals ($pd\sigma$) and ($pd\pi$).¹⁰ The Hamiltonian for the double cluster, FeTiO_9 , is chosen as a straight extension of the conventional type for the single cluster, TiO_6 , and is given by

$$H = H_{\text{Ti}} + H_{\text{O}} + H_{\text{Ti-O}} + H_{\text{Fe}} + H_{\text{Fe-O}} + H_{\text{Fe-Ti}}, \quad (2)$$

where the first H_{Ti} , H_{O} , and $H_{\text{Ti-O}}$ terms in the right-hand side represent the same interactions as mentioned above, while the last term $H_{\text{Fe-Ti}}$ is additionally introduced in the double-cluster model and describes the Fe $3d$ -Ti $3d$ intermetallic charge transfer given in terms of transfer integrals ($dd\sigma$), ($dd\pi$), and ($dd\delta$). As in the conventional treatment, the parameters related to the full-multiplet interactions are numerically estimated from the atomic calculation within the Hartree-Fock-Slater scheme,¹¹ while the other parameters defined above are treated as adjustable ones.

The ground state (GS) and the RIXS final state for the TiO_6 cluster are described as a linear combination of basis configurations d^0 , $d^1\bar{L}$, and $d^2\bar{L}^2$. On the other hand, those for the FeTiO_9 cluster are described as a linear combination of d^6d^0 , d^5d^1 , $d^7d^0\bar{L}^1$, $d^6d^1\bar{L}^1$, $d^5d^2\bar{L}^1$, $d^8d^0\bar{L}^2$, $d^7d^1\bar{L}^2$, and $d^6d^2\bar{L}^2$, where $d^l d^m \bar{L}^n$ denotes the electronic configuration with $(3d)^l$ in Fe, $(3d)^m$ in Ti, and n holes in oxygen ligands, i.e., starting from the configuration in nominal-valence Fe^{2+} , Ti^{4+} , and filled oxygen ligands, we take into account configurations successively generated by $3d$ - $2p$ and $3d$ - $3d$ charge transfer. The $2p$ XAS final state or RIXS intermediate state is described by a linear combination of the basis configurations, which are obtained merely by adding a $2p$ core hole and a $3d$ electron to the ground-state basis configurations.

The model Hamiltonian in Eqs. (1) and (2) is numerically diagonalized. The $2p$ XAS is obtained according to the Fermi golden rule, while RIXS is obtained according to the Kramers-Heisenberg formula. The values of adjustable parameters in the present study are listed in Ref. 12.

Figure 2 shows the calculated Ti $2p$ RIXS in (a) the single-cluster model and (b) the double-cluster model as a function of energy loss. The calculated XAS of each model is shown in the top panels and the line shape is in agreement with previously reported ones for Ti^{4+} oxides.^{3,6} The capital letters in the spectra correspond to the letters in Fig. 1. The origin of these peaks in the range of -5 – -10 eV is interpreted to be the charge transfer from O $2p$ to Ti $3d$. The low-energy satellites α and β , in the energy range of -2 – -5 eV, clearly arise only in the double-cluster model [Fig. 2(b)] and not in the single-cluster model [Fig. 2(a)]. In Fig. 1, the α and β peaks appear at lower energy excitation resonances and are enhanced when the excitation energy is at the

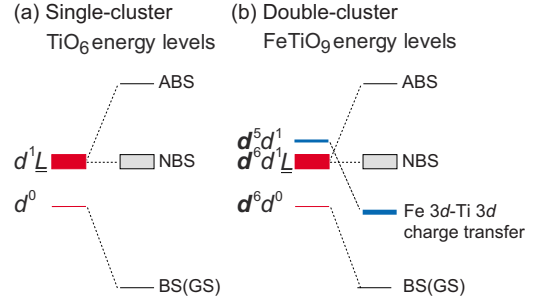


FIG. 3. (Color online) Energy diagrams of the lowest bases for the initial state for the RIXS for (a) the single-cluster model and (b) the double-cluster model. GS: ground state; BS: bonding state; ABS: antibonding state; NBS: nonbonding $3d^1\bar{L}$ state. \bar{L} denotes a ligand hole and $d^l d^m \bar{L}^n$ is the configuration of $\text{Fe}(3d^l)$, $\text{Ti}(3d^m)$, and n holes at the oxygen ligands.

higher energy absorption peaks. In particular, the α peak clearly appears when excitation is at the peak B of XAS, which is assigned to e_g symmetry. At a higher incident energy, at absorption resonance D, which is assigned to e_g symmetry, both peaks α and β are enhanced. This behavior is well reproduced in the calculated spectra in Fig. 2(b) for the double-cluster model. Using the results from the theoretical calculation, we interpret the experimental results.

The energy diagrams of the RIXS process for the single- and double-cluster models are shown schematically in Fig. 3, where only the lowest bases for the initial state are included for simplicity. The antibonding states (ABSs) would appear at higher RIXS energy losses and are not shown in Fig. 2. The structures in the calculated spectrum in the energy region between -10 and -5 eV in Fig. 2, in principle, correspond to the observed RIXS structure in the same energy region in Fig. 1. These features are attributed to the transitions to nonbonding $3d^1\bar{L}$ states (NBSs), which are denoted by rectangles in Fig. 3 in both the single- and double-cluster energy schemes. These structures appear when the charge transfer from O $2p$ to Ti $3d$ occurs regardless of whether the model includes the contribution from the Fe $3d$ state or not. As shown in the schematic including only Ti $3d$ -O $2p$ bonding, there are no states between the ground state and the NBS. However, when the Fe $3d$ -Ti $3d$ charge transfer (d^5d^1) is included, an additional state arises in between the GS and the NBS, as shown by the thick bar in Fig. 3(b).

Among the numerous studies of $3d^0$ transition-metal compounds, the low-energy-loss peaks have occasionally been interpreted in terms of a possible admixture of the Ti^{3+} ion arising from stoichiometry deviations. However, as we mentioned before, the present feature behaves differently upon changing the incident energy. Furthermore, even if an impurity-level Ti^{3+} admixture were present in the grown single crystal owing to some stoichiometry deviation, it would not yield spectral features with intensities comparable to those related to the O $2p$ -TM $3d$ hybridization. Therefore, on the basis of the comparison of the experimental observations and the results of calculations using the double-cluster model including the Fe $3d$ -Ti $3d$ intermetallic charge transfer, which is expressed by the $H_{\text{Fe-Ti}}$ term in Eq. (2), we conclude that the intermetallic charge transfer indeed occurs

in FeTiO₃. In manganites [viz. LaMnO₃ and (La,Sr)MnO₄] the Mn atom is octahedrally coordinated by the ligand oxygens, and two neighboring octahedra always share only one oxygen at a corresponding vertex (“corner-sharing perovskite”). The orbital overlap, and thus even the intersite *d-d* charge transfer, then proceeds via the (hybridized) oxygen *2p* states, rather than being due to a pristine intermetallic orbital overlap. In ilmenite, on the other hand, the oxygen octahedra are face sharing, and the intermetallic orbital overlap can occur directly, because the oxygen then is not separating the metal atoms. With that in mind, the direct (nonmediated) intermetallic interaction component was included in the calculation, which indeed, as displayed in Fig. 2, causes the calculation to reproduce the spectral features at low energy loss. In the wording “intersite *d-d* charge transfer,” which has already been used in several studies^{13–16} the mediator O *2p* orbitals had been tacitly assumed, which in our case might mislead the reader since what we have identified in the spectra is the effect of exactly the absence of such mediator oxygen orbitals in the intersite *d-d* charge transfer. This conclusion is supported by molecular-orbital calculations for the (FeTiO₁₀)¹⁴⁻ cluster, which predict the chemical state of Fe-Ti interaction in the energy region.¹⁷

In summary, we have compared our experimental FeTiO₃

Ti *2p* RIXS spectra against the single-cluster (Ti with oxygen ligands) and double-cluster (adjacent Ti and Fe with their oxygen ligands) models and found that only the double-cluster model with intermetallic charge transfer reproduces the experimental results adequately, whereas the more conventional single-cluster approach fails to reproduce several indicative features completely. From this difference between the theoretical results the single and double models, i.e., the existence of intermetallic charge transfer, we found evidence of the direct (i.e., not mediated by oxygen) TM *3d*-TM *3d* interaction. Our experimental spectra indicate the intermetallic charge transfer, the importance of which has previously been underestimated, and often neglected, to be of the same scale as the outcome of the known anion-cation charge transfer. We expect that intermetallic charge transfer is an additional key to understanding the physical properties of TM oxide compounds.

We would like to thank A. Ito for sample preparation and J. Nordgren for his encouragement during the experiments. The experimental work was performed at MAX-lab in Sweden. We gratefully acknowledge the MAX-lab staff for working conditions at the beam line.

*agui@spring8.or.jp

¹H. Kato, M. Yamada, H. Yamauchi, H. Hiroyoshi, H. Takei, and H. Watanabe, *J. Phys. Soc. Jpn.* **51**, 1769 (1982).

²A. Kotani and S. Shin, *Rev. Mod. Phys.* **73**, 203 (2001).

³S. M. Butorin, J.-H. Guo, M. Magnuson, and J. Nordgren, *Phys. Rev. B* **55**, 4242 (1997).

⁴M. Matsubara, T. Uozumi, A. Kotani, Y. Harada, and S. Shin, *J. Phys. Soc. Jpn.* **69**, 1558 (2000).

⁵J. Nordgren, G. Bray, S. Cramm, R. Nyholm, J.-E. Rubensson, and N. Wassdahl, *Rev. Sci. Instrum.* **60**, 1690 (1989).

⁶F. M. F. de Groot, J. C. Fuggle, B. T. Thole, and G. A. Sawatzky, *Phys. Rev. B* **41**, 928 (1990).

⁷C. Ulrich, G. Ghiringhelli, A. Piazzalunga, L. Braicovich, N. B. Brookes, H. Roth, T. Lorenz, and B. Keimer, *Phys. Rev. B* **77**, 113102 (2008).

⁸T. Higuchi, T. Tsukamoto, M. Watanabe, M. M. Grush, T. A. Callcott, R. C. Perera, D. L. Ederer, Y. Tokura, Y. Harada, Y. Tezuka, and S. Shin, *Phys. Rev. B* **60**, 7711 (1999).

⁹A. Augustsson, A. Henningsson, S. M. Butorin, H. Siegbahn, J. Nordgren, and J.-H. Guo, *J. Chem. Phys.* **119**, 3983 (2003).

¹⁰J. C. Slater and G. F. Koster, *Phys. Rev.* **94**, 1498-1524 (1954).

¹¹H. D. Cowan, *The Theory of Atomic Structure and Spectra* (Uni-

versity of California Press, Berkeley, 1981).

¹²TM *3d*-O *2p* charge-transfer energy: $\Delta(\text{Ti})=3.0$ eV and $\Delta(\text{Fe})=5.5$ eV. Crystal-field energy: $10Dq=1.5$ eV and $a=0.3$ eV for Ti, $10Dq=0.5$ eV and $a=0.1$ eV for Fe, where $a=Ed(a_{1g})-Ed(e_{g\pi})$. *3d* Coulomb: $U_{dd}(\text{Ti})=4.5$ eV and $U_{dd}(\text{Fe})=7.0$ eV. *2p* core-hole potential: $U_{dc}(\text{Ti})=6.0$ eV and $U_{dc}(\text{Fe})=8.0$ eV. TM *3d*-O *2p* hybridization: $pd\sigma=-1.7$ eV for Ti and $pd\sigma=-1.3$ eV for Fe. Ti *3d*-Fe *3d* hybridization: $dd\sigma: dd\pi: dd\delta=-1.0: 0.5: 0.2$ eV and $dd\sigma=-0.4$ eV. The calculation is performed under D_{3d} symmetry using ($pd\sigma$).

¹³N. N. Kovaleva, A. V. Boris, C. Bernhard, A. Kulakov, A. Pimenov, A. M. Balbashov, G. Khaliullin, and B. Keimer, *Phys. Rev. Lett.* **93**, 147204 (2004).

¹⁴S. Grenier, J. P. Hill, V. Kiryukhin, W. Ku, Y.-J. Kim, K. J. Thomas, S.-W. Cheong, Y. Tokura, Y. Tomioka, D. Casa, and T. Gog, *Phys. Rev. Lett.* **94**, 047203 (2005).

¹⁵A. Gössling, M. W. Haverkort, M. Benomar, H. Wu, D. Senff, T. Möller, M. Braden, J. A. Mydosh, and M. Grüninger, *Phys. Rev. B* **77**, 035109 (2008).

¹⁶T. Ide and A. Kotani, *J. Phys. Soc. Jpn.* **69**, 1895 (2000).

¹⁷D. M. Sherman, *Phys. Chem. Miner.* **14**, 364 (1987).